Transitions amongst synchronous solutions for the stochastic Kuramoto model

Lee DeVille
University of Illinois

July 20, 2011

Abstract

We consider the Kuramoto model of coupled oscillators with nearest-neighbor coupling and additive white noise. We show that synchronous solutions which are stable without the addition of noise become metastable and that we have transitions amongst synchronous solutions on long timescales. We compute these timescales and, moreover, compute the most likely path in phase space that transitions will follow. The timescales do not increase as the number of oscillators in the system increases and are roughly constant in the system size. The transitions correspond to a splitting of one synchronous solution into two communities which move independently for some time and which rejoin to form a different synchronous solution.

1 Introduction

The study of the propensity of coupled systems to synchronize has had a long history that has inspired many of the ideas in modern dynamical systems theory and in statistical physics. The specific study of oscillator synchronization has done much to explain the dynamics of many real systems, including cardiac rhythms [1–3], circadian rhythms [4, 5], biochemical kinetics and excitable media [6–11], earthquakes [12–14], a wide variety of neural systems [15–25], and even synchronization of fireflies [26–28]. See [29–31] for reviews.

One of the most studied examples of synchronization is the Kuramoto model [11, 32]; for some reviews and similar models see [31, 33, 34]. One of the reasons for the study of this particular model is its relative simplicity and analytic tractability; however, even a simple model such as this gives rise to a staggering amount of complexity. It is also considered a reasonable phenomenological model for various biological and physical processes in superconductivity [35, 35] and neuroscience [36–39] (see [40] and the reviews mentioned above for more examples).

The original theoretical success of the Kuramoto model is that its synchronization properties in the $N \to \infty$ limit can be understood using ideas from statistical physics [32, 40–44]. Most studies for finite N have concentrated on the existence (or lack thereof) of synchronous solutions [45–50], although there has been at least one study concerning the interaction of multiple synchronous solutions [51]. Stochastic perturbations of the Kuramoto system have been studied [15, 52–54] (also see [55, 56]) with a view towards understanding their propensity to facilitate synchronization.

At the same time and more broadly, there has been a large body of work in both the statistical physics and mathematics communities on the broader questions involving synchronization of interacting elements and the wide variety of dynamics such coupled systems can display [57–65]. There has also been significant interest in understanding the effect of noise on such coupled systems [66–75]. In these examples, depending on the context, it is useful to either think of the noise as unresolved degrees of freedom of a complex system (most common in statistical physics approaches) or instead as a complex exogenous input to an open system (more common in biology, esp. neuroscience).

One of the nice properties a dynamical system gains when it is perturbed by noise is (under mild conditions) ergodicity and the existence of a unique invariant measure; together these can completely describe the system. However, even this has limitations, since the invariant measure is guaranteed to only give information when the system is considered over an infinite time interval. In general, such systems can exhibit metastability which traps them in some subset of the phase space for long but finite times. The original study of such questions in the limit of small stochastic perturbations is what is now known as the Freidlin-Wentzell (FW) theory [76–82], which built upon the earlier successes of large deviation theory [83–85]. This theory has had a large success being applied to specific applied problems in recent years [86–93]. The main moral of the FW theory is that if we perturb a dynamical system with small noise, then it will spend most of its time near the attracting structures of this dynamical system, then make rare excursions amongst these structures on long timescales (where "long" here will mean timescales which scale exponentially long in the size of the noise). The FW theory allows us to compute the typical timescales of such excursions and their typical shape.

The purpose of this paper is to study the Kuramoto oscillator when perturbed by noise and understand the long timescale behavior of this system, specifically through an application of the FW theory. We consider a case where there are multiple synchronous solutions and compute the likely transitions amongst these. It should be noted that the Kuramoto system has the property that stable configurations arise only through the interaction, and in general the individual oscillators do not have an internal stationary state.

In particular, we show how if one perturbs a "synchronizable" Kuramoto model by noise, then instead of observing one (or multiple) stable stationary configurations, the noisy system will transition amongst these configurations. These transitions have the qualitative form that some community of the oscillators breaks off, wraps around the system, and then forms a new stable configuration. Moreover, we can compute the timescales on which such transitions should occur and details of their dynamics during the transition. This paper can be thought of as something like an "orthogonal complement" to [51]: there what was studied was the "width" of the "sync basin", i.e. how many initial conditions fall into the basin of attraction of the most stable synchronous solution; this paper is, in this light, a study of the "depth" of this sync basin and how hard it is for the system to crawl out.

The rest of the paper is organized as follows. In Section 2 we give a statement of the problem we consider, present a concise overview of the results of the paper, and present some numerical simulations of the system. In Section 3, we review the relevant components of the FW theory and present precise statements of the theorems which we prove. We delay the proofs of these theorems to Section 4. Finally, we give some concluding remarks in Section 5 and discuss some possible generalizations of the current approach.

2 Results

This section is a quick overview of the remainder of the paper. In Section 2.1 we motivate and present the problem that we consider. In Section 2.2 we give intuitive overviews of the results of the paper. Finally, in Section 2.3, we present a series of numerical computations.

2.1 Statement of the problem

The standard formation of the deterministic Kuramoto problem is as follows. Consider a weighted (directed) graph $\Gamma = (V, E)$ and denote γ_{ij} as the weight of edge $i \to j$. For any $\omega \in \mathbb{R}^N$, define the dynamical system on $\theta \in \mathbb{T}^N$ by

$$\frac{d\theta_i}{dt} = \omega_i + \sum_j \gamma_{ji} \sin(\theta_j - \theta_i). \tag{1}$$

One stochastic generalization of (1) would be to consider an SDE whose drift term corresponds to (1), namely

$$d\theta_i = (\omega_i + \sum_j \gamma_{ji} \sin(\theta_j - \theta_i))\, dt + \sigma(\boldsymbol{\theta})\, dW_t^{(i)}. \tag{2}$$

Two common choices of interaction graphs are the all-to-all network $\gamma_{ij} = K/N$ or the nearest neighbor network $\gamma_{ij} = K(\delta_{j,i+1} + \delta_{j,i-1})$. We will concentrate on the case of nearest-neighbor symmetric coupling and additive noise, i.e. we consider

$$d\theta_n = \{\omega_n + K\left[\sin(\theta_{n+1} - \theta_n) + \sin(\theta_{n-1} - \theta_n)\right]\}\, dt + \sqrt{2\epsilon}\, dW_t^{(n)}, \tag{3}$$

where we choose N not a multiple of 4. As we discuss further in Section 5, the methods we use in this paper are applicable to any interaction graph Γ, although different Γ would give rise to different specific computations throughout. We actually choose nearest-neighbor because this is the case which gives the richest possible structures (see Section 5), and we choose N not a multiple of 4 for technical reasons which we describe in Lemma 4.1 and Remark 4.2.

As is well known, (3) is invariant under two different group actions[1], one continuous and one discrete, namely:

$$\boldsymbol{\theta} \mapsto \boldsymbol{\theta} + C\mathbf{1}, \quad \boldsymbol{\theta} \mapsto \boldsymbol{\theta} + 2\pi\mathbb{Z}^N. \tag{4}$$

There are several ways to deal with the continuous group action which are usually not distinguished in the deterministic case, but which matter here. The choice we make here is done for the purposes of simplicity in notation and presentation, namely: we pin one of the oscillators at 0, thus adding a Dirichlet-like boundary condition to the system:

$$d\theta_n = \{\omega_n + K\left[\sin(\theta_{n+1} - \theta_n) + \sin(\theta_{n-1} - \theta_n)\right]\}\, dt + \sqrt{2\epsilon}\, dW_t^{(n)}, \quad \theta_0 = 0. \tag{5}$$

where $\theta_n \in [0, 2\pi)$, $dW^{(n)}$ are independent Brownian motions, and $n = 1, \ldots, N-1$. To simplify the notation we write $\theta_N := \theta_0$. This system now has $N-1$ degrees of freedom, since we have pinned one oscillator. It is a small stochastic perturbation of the system

$$\frac{d\theta_n}{dt} = \omega_n + K\left[\sin(\theta_{n+1} - \theta_n) + \sin(\theta_{n-1} - \theta_n)\right], n = 1, \ldots, N-1, \quad \theta_0 = 0. \tag{6}$$

There are alternate ways we could have dealt with the continuous group action which we discuss in Section 5 below.

2.2 Summary of results of paper

To state our results we will need to introduce some notation. Solutions of (6) are invariant under translations in the lattice $2\pi\mathbb{Z}^{N-1}$. We define the projection

$$\begin{aligned} \Pi\colon \{0\} \times \mathbb{R}^{N-1} &\to \{0\} \times \mathbb{R}^{N-1}/2\pi\mathbb{Z}^{N-1}, \\ \{\theta_i\}_i &\mapsto \{\theta_i \pmod{2\pi}\}_i \end{aligned} \tag{7}$$

and the associated equivalence relation $[\cdot]$ on fibers. In particular, we have

$$[\mathbf{0}] = [(0, 0, \ldots, 0)] = \{(0, 2\pi\ell_1, \ldots, 2\pi\ell_{N-1}) \mid \ell_k \in \mathbb{Z}\}.$$

It will be convenient below to specify a fundamental domain for the discrete action, so we choose

$$D_N := \{0\} \times [0, 2\pi)^{N-1} \subseteq \{0\} \times \mathbb{R}^{N-1}. \tag{8}$$

Finally, for simplicity of notation below, we define $\mathbf{e}_k$ as the kth standard basis vector in $\mathbb{R}^N$ and define

$$\mathbf{f}_k = \sum_{l>k} \mathbf{e}_l. \tag{9}$$

We are now ready to state the results of the paper. For an open set of $\boldsymbol{\omega}$ containing $\boldsymbol{\omega} = \mathbf{0}$:

- System (5) will spend most of its time in a small neighborhood of $[\boldsymbol{\theta}^*]$, where $\boldsymbol{\theta}^* = \boldsymbol{\theta}^*(\boldsymbol{\omega}) \in D_N$ is an attracting fixed point, and $\boldsymbol{\theta}^*(\mathbf{0}) = \mathbf{0}$. ($\boldsymbol{\theta}^*(\boldsymbol{\omega})$ is in some sense the "most" attracting fixed point, see below.) More specifically, given a fixed open neighborhood $U \ni [\mathbf{0}]$ which is small enough and invariant under the $2\pi\mathbb{Z}^{N-1}$ action, there is a $C > 0$ such that the proportion of time (5) spends in U^c scales like $e^{-C/\epsilon}$ as $\epsilon \to 0$. This C depends on U but not on the initial condition.
- System (5) will make rare but rapid excursions between different elements of $[\mathbf{0}]$. More specifically, if we choose U' any open subset of U with $\overline{U'} \subsetneq U$, then whenever (5) enters U', it will remain inside U for a random time whose mean scales like $e^{C'/\epsilon}$ for some fixed $C' > 0$ and which is distributed exponentially. Moreover, this C' can be computed exactly. Finally, the time it takes to make a transition between when the system exits U and enters U' has a mean which exponentially smaller than the residence time inside U'.

[1]When we say a stochastic process X_t is invariant under a group action, we simply mean that there is a group G so that $\mathbb{P}(X_t \in A|X_0 = x) = \mathbb{P}(X_t \in gA|X_0 = gx)$ for all $g \in G$.

- The most likely path of transition between elements of $[\mathbf{0}]$ can be computed for ϵ small; that is to say, when these rare transitions occur, they will do so, with high probability, in a small neighborhood of particular paths in the phase space. Moreover, these paths correspond to some community of the oscillators peeling off from the main pack, traversing the circle, and then rejoining the pack in a new synchronous collection (q.v. Remark 4.5).

In particular, we can state explicitly all of the cases where $\boldsymbol{\omega} = \mathbf{0}$, if we define τ to be the typical time that system (5) sits near an element of $[\mathbf{0}]$ before making a transition, then we show below that[2] for each N not divisible by 4,

$$\tau \asymp \exp(I_N/\epsilon),$$

where

$$I_N := K\left[N - (N-1)\cos\left(\frac{\pi}{N-2}\right) + \cos\left(\frac{N-3}{N-2}\pi\right)\right]. \tag{10}$$

We can also describe the path which the system takes through phase space from one element of $[\mathbf{0}]$ to another. Choose, for example, $z_1 = \mathbf{0}$ and $z_5 = 2\pi\mathbf{f}_k$ for some k. Then there are five distinguished points: the two points $\mathbf{0}, z_1$, the point z_3 which is a local sink and is formed by placing N oscillators on the circle with equal spacing and in order, and two saddles z_2, z_4, each of which can be constructed by placing $N+1$ oscillators on the circle with equal spacing, and then removing one. Then a path from z_1 to z_5 will be close to a path which passes $z_1 \to z_2 \to z_3 \to z_4 \to z_5$. Moreover, the number I_N is related to the points z_2 and z_4 in a specific sense (being the "relative energy" of $z_{2,4}$ compared to $z_{1,5}$, in a sense to be made precise below). Moreover, all transition paths from one element of $[\mathbf{0}]$ to another is either a path like those described above or a concatenation of such paths.

2.3 Numerical results

We present two sets of simulations of the solutions of (5) below, demonstrating that the system spends almost of all its time in a neighborhood of $[\mathbf{0}]$, and makes rare excursions between elements of this set. All simulations below use a first-order Euler-Maruyama method for 5 with timestep $\Delta t = 10^{-1}$.

In Figure 1 we present one realization of the system with $N = 3, \epsilon = 0.1, K = 0.1$. We have plotted the actual solution in blue and the elements of $[\mathbf{0}]$ as red circles. We can see that there is a neighborhood of $[\mathbf{0}]$ in which the system spends almost all of its time; otherwise the system makes rare excursions amongst these.

In Figure 2 we are plotting trajectories of (5) versus time for $N = 5$ and $N = 17$. We see again that the system spends most of its time in a small neighborhood of $[\mathbf{0}]$; here we can also obtain a sense of the residence time that the system spends in a state between transitions. It is clear from these graphs that these residence times are random and quite irregular; e.g. in the $N = 5$ case it is clear to the eye that these residence times range over at least an order of magnitude. One of the consequences of Theorem 3.4 is that these residence times are distributed exponentially (we will present histograms of these times in Figure 4 below).

3 Analysis and Statements of Theorems

This purpose of this section is to state the theorems and main results of the paper precisely. Here we do two things: in Section 3.1 we give an overview of the classical results of the FW large deviation theory [76] which we will use; in Section 3.2 we state the results specific to this paper. Speaking loosely, in Section 3.1 we explain what it is we need to compute and why, and in Section 3.2 we explain the results of the computations for the system considered here.

3.1 FW Theory

The well-known FW theory [76] describes the behavior of stochastic processes which can be written as small stochastic perturbations of deterministic dynamical systems, and the main conclusions can be sum-

[2] We say that $a(\epsilon) \asymp b(\epsilon)$ if $\lim_{\epsilon\to 0} \dfrac{\log(a(\epsilon))}{\log(b(\epsilon))} \in (0,\infty)$.

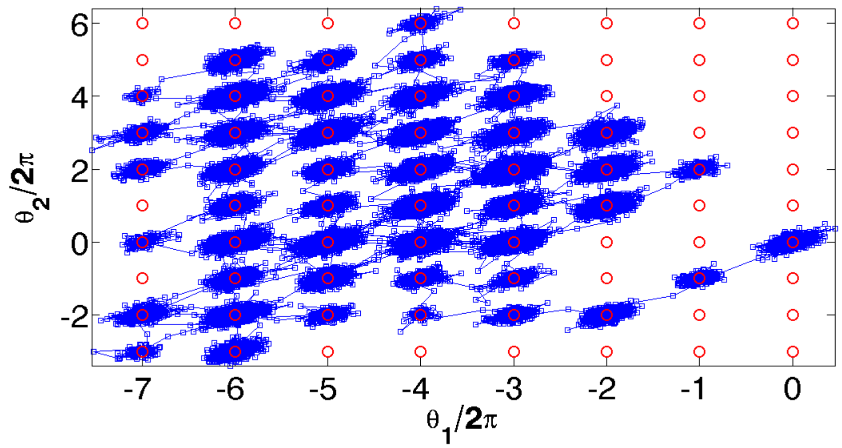

Figure 1: One realization of (5) with $N = 3$, $\epsilon = 0.1$, $K = 0.1$. We have placed red circles at elements of $[\mathbf{0}]$. As predicted, the system spends almost all of its time near these translates of the origin, and makes rare excursions between these points. This system was run until $t = 10^6$.

marized as follows. We give a brief overview of this theory here for completeness[3]. An SDE of the form

$$dX_t^\epsilon = b(X_t^\epsilon)\,dt + \sqrt{2\epsilon}\sigma(X_t^\epsilon)\,dW_t \tag{11}$$

will spend most of its time between the stable structures of the deterministic ODE

$$\frac{dx}{dt} = b(x), \tag{12}$$

and process (11) will make transitions between these stable structures on exponentially long timescales. The statements can be made much more concrete and specific when the underlying deterministic dynamical system is a gradient system whose attracting set is a discrete union of attracting fixed points and the stochastic perturbation is additive white noise, and this is what we will state precisely below. We first introduce some terminology.

Definition 3.1. *Consider an ODE on $\mathbb{R}^N$. An n-saddle is a hyperbolic fixed point whose Jacobian has exactly n eigenvalues with positive real part. We will call 0-saddles* **sinks** *and N-saddles* **sources***. If x, y are two fixed points, we say that x* **leads to** *y ($x \to y$) if the unstable manifold of x intersects with the stable manifold of y, i.e. if there is a trajectory of the system $z(t)$ with $\lim_{t\to-\infty} z(t) = x$ and $\lim_{t\to\infty} z(t) = y$. We will say the* **sinks** *x_1, x_2* **are connected by the saddle** *y if x_1, x_2 are sinks, y is a 1-saddle, and $y \to x_1, y \to x_2$.*

Notice that if x_1 and x_2 are connected by y, then since y is a 1-saddle, it has a one-dimensional unstable manifold, so that in one direction is approaches x_1 and in the other x_2; in short, any small perturbation of y will go to either x_1 or x_2 as $t \to \infty$. One of the main results of [76] is that all we need to know to really understand the behavior of system (5) is the local neighborhoods of the sinks, the local neighborhoods of the 1-saddles, and which sinks are connected by which 1-saddles for system (6). More specifically, consider a gradient system of the form

$$dX_t^\epsilon = -\nabla V(X_t^\epsilon)\,dt + \sqrt{2\epsilon}\,dW_t, \tag{13}$$

where $X_t^\epsilon \in \mathbb{R}^N$, $V\colon \mathbb{R}^N \to \mathbb{R}$ is C^2 such that $V(x) \to \infty$ as $|x| \to \infty$ fast enough[4], and dW_t is N-dimensional white noise. Assume that the attractor of V is a discrete union of attracting fixed points, and denote the attracting fixed points by $z_1, \ldots, z_M$. It is not hard to verify that the unique invariant measure $\mu^\epsilon(dx)$ has the Gibbs distribution

$$\mu^\epsilon(dx) = \rho^\epsilon(x)\,dx := Z^{-1}\exp(-V(x)/\epsilon), \tag{14}$$

[3] a very well-written and accessible alternate exposition is contained in Section 2.2 of [88]

[4] $V(x) = O(|x|)$ is fast enough—what we need here is that V has compact level sets and that the Gibbs distribution is well-defined

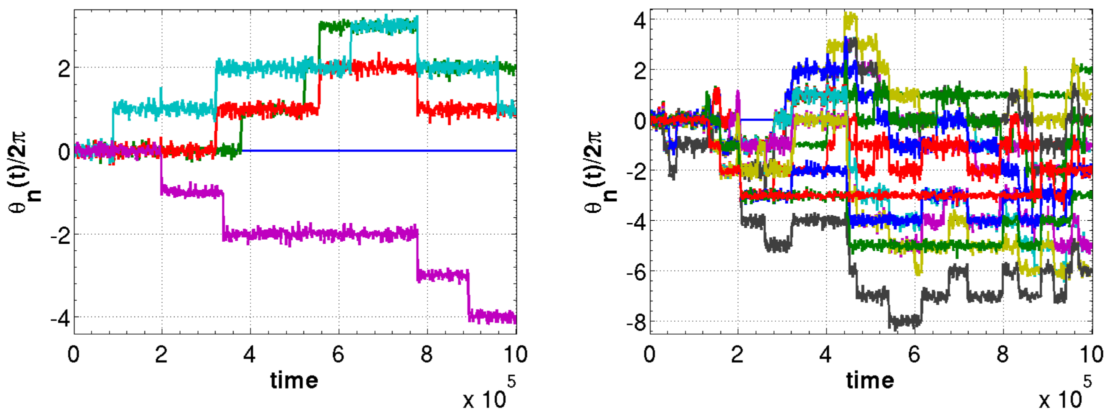

Figure 2: Realization of (5) for $N = 5$ (left panel) and $N = 17$ (right panel). For the $N = 5$ case, we have chosen $K = 0.1, \epsilon = 0.06$, and for the $N = 17$ case we have chosen $K = 0.1, \epsilon = 0.05$.

where Z is chosen so that $\int_{\mathbb{R}^N} \mu^\epsilon(dx) = 1$. Note that this measure has a density, i.e. is absolutely continuous with respect to the Lebesgue measure. From this, we first note that (13) spends the vast majority of its time in a neighborhood of $\cup_{m=1}^M z_m$; more specifically, given any open neighborhood U of $\cup_{m=1}^M z_m$, then there exists a constant C with

$$\mu^\epsilon(U^c) \asymp e^{-C/\epsilon}. \tag{15}$$

Moreover, the system will spend more time near the "deeper" fixed points: namely, if we choose $U_m \ni z_m$ open, then

$$\mu^\epsilon(U_m) \asymp \exp(\epsilon^{-1}(V(z_m) - V^*)),$$

where $V^* := \min_m V(z_m)$. In particular, if there is a fixed point with energy strictly less than all of the others, then the system will spend an exponentially small amount of time outside a neighborhood of this point.

These statements about the invariant measure do not tell us much about the dynamics; for example, the system spends almost all of its time near attracting fixed points, but if we converge to a unique measure then there must be transitions amongst these points. The transitions between these attracting fixed points occur on exponentially long timescales. Consider two attracting fixed points z, z' which are at the minimum energy $V(z) = V(z') = V^*$ and which are connected by the n 1-saddles $y_1, \ldots, y_n$. For the saddle y_k, denote by U_k an open tubular neighborhood of the union of two deterministic trajectories, the first being the (infinite-time) downhill trajectory from y_k to z, and the other being the trajectory from y_k to z'. Choose V a small open neighborhood of z'. Then [76, Theorems 4.2.1, 4.4.1],

$$\tau := \min_{t>0}\{X_t \in V | X_0 = z\} \asymp \exp\left(\epsilon^{-1} \min_{i=1,\ldots,n} V(y_i)\right). \tag{16}$$

Moreover, if we let Q be the set of 1-saddles with minimum energy, i.e. $q \in Q$ if and only if $V(y_q) = \min_{i=1,\ldots,n} V(y_i)$, then there is a constant $C > 0$ such that

$$\mathbb{P}\left[X_t \notin \cup_{q\in Q} U_q\right] \asymp e^{-C/\epsilon}.$$

In short, to compute the transition time from z to z', we find all 1-saddles which connect z, z', and find which one of those has minimum energy, call this energy $I_{z,z'}$. Then the timescale of transition is $\exp(\epsilon^{-1} I_{z,z'})$. If the minimum energy saddle is unique, then the system will pass near that saddle during the transition; if not, and there is a set of saddles with the same minimum energy, then the system will pass near one of them.

In short, to understand the small-noise asymptotics of a system of type (13), we need only compute two particular graphs Γ_1, Γ_2. Let Γ_1 be the weighted undirected bipartite graph (A, B, E_1) where A is the set of sinks, B the set of 1-saddles, and we say that $(x, y) \in E_1$ if y leads to x. The weight on edge (x, y) is the positive real number $w_{xy} := V(y) - V(x)$. Define Γ_2 as the weighted directed bipartite graph (A, E_2) where A is again the set of sinks of (13), and we say that

$$x_1 \to x_2 \in E_2 \iff (x_1, y) \in E_1, (x_2, y) \in E_1 \text{ for some } y \in B.$$

Moreover, we define the weight

$$w_{x_1 \to x_2} := \min_{y | (x_1, y), (x_2, y) \in E_1} V(y) - V(x_1).$$

(Notice by definition that Γ_2 is directed, but only because of the weights; the underlying connection topology of Γ_2 is symmetric.) Then [76, Theorem 6.5.2], we can approximate the dynamics of (13) by a continuous time Markov chain whose underlying transition graph is the same as Γ_2, and where the rate of transition from x_1 to x_2 is given by $\exp(\epsilon^{-1} w_{x_1 \to x_2})$, i.e. consider the transition matrix Q on the sinks where

$$Q_{x_i, x_j} = \begin{cases} \exp(\epsilon^{-1} w_{x_i \to x_j}), & (x_i \to x_j) \in E_2, \\ 0, & \text{else}, \end{cases}, \text{ if } i \neq j,$$
$$Q_{x_i, x_i} = \sum_{j \neq i, x_j \in A} Q_{x_i, x_j}.$$

Finally, if we have two sinks x_i, x_j which are not connected by a saddle, then they are not connected by an edge in Γ_2, but they could be connected by a path in Γ_2 (and in general, they will be generically if V is proper). However, note that if $a > b$, then $e^{-a/\epsilon} \ll e^{-b/\epsilon}$. The consequence of this is that if we want to compute the expected transition time from one minimum to another, we consider all paths connecting these two in Γ_2; for each path, consider the maximum weight along that path, and then minimize over all paths.

We mention that one can be more precise than (16), using the Kramers-Eyring formula [79,80,90,94,95]. Assume the minimum energy connecting saddle is unique and denote it by y, then

$$\mathbb{E}[\tau] = \frac{2\pi}{\sqrt{\lambda_1(y)}} \sqrt{\frac{\det \nabla^2 V(y)}{\det \nabla^2 V(z)}} e^{V(y) - V(z)/\epsilon} (1 + o(1)), \tag{17}$$

where $\lambda_1(y)$ is the unique positive eigenvalue of $\nabla^2 V(y)$. We will not need the more precise asymptotics here, since, as we see below, there will be a unique class of 1-saddles which have the minimum action and these corrections would not distinguish amongst them. Of course, as a predictor of transition times, (17) gives a better approximation than (16).

3.2 Statement of theorems

We will give an overview of the results in this paper by developing and stating the three main theorems of the paper. We delay the proofs of these theorems until Section 4.

We will show below that for $N > 4$ and some choices of $\boldsymbol{\omega}$, there are multiple attracting fixed points in the fundamental domain D_N. Moreover, we need to know their relative depths and thus we need to know the potential in which they flow. Thus we define

$$V_{\boldsymbol{\omega}}(\boldsymbol{\theta}) = KN - \sum_{i=1}^{N-1} (\omega_i \theta_i + K \cos(\theta_{i+1} - \theta_i)), \tag{18}$$

where we denote $\theta_N = \theta_0$. It is easy to check that $-\nabla V_{\boldsymbol{\omega}}$ is the right-hand side of (6). Moreover, in the case where $\boldsymbol{\omega} = \mathbf{0}$, we have

$$V(\boldsymbol{\theta}) := V_{\mathbf{0}}(\boldsymbol{\theta}) = K(N - \sum_{i=1}^{N} \cos(\theta_{i+1} - \theta_i)). \tag{19}$$

We choose the constant term so that $V_{\mathbf{0}}(\mathbf{0}) = 0$. Note that for $\boldsymbol{\omega} = \mathbf{0}$, a constant factor of K pulls out of formula (19).

We need to find the sinks and 1-saddles of (6), and we can find an explicit formula when $\boldsymbol{\omega} = \mathbf{0}$.

Definition 3.2. *We define* $\mathbf{s}_N(\alpha)$ *and* $\mathbf{t}_N^{(k)}(\alpha)$ *as the vectors in* $\mathbb{R}^N$ *with coordinates*

$$\begin{aligned}(\mathbf{s}_N(\alpha))_\ell &:= \ell\alpha, \quad \ell = 0, \ldots, N-1,\\ \left(\mathbf{t}_N^{(k)}(\alpha)\right)_\ell &:= \begin{cases}\ell\alpha, & \ell = 0, \ldots, k-1,\\ \pi + (\ell - k)\alpha, & \ell = k, \ldots, N-1.\end{cases}\end{aligned} \tag{20}$$

Theorem 3.1. *Choose* $N > 4$ *and* $N \neq 0 \pmod 4$ *and* $\boldsymbol{\omega} = \mathbf{0}$*. The sinks and 1-saddles of* (6) *lying in the fundamental domain* D_N *are:*

- *The sinks are* $\mathbf{s}_N(\alpha)$ *with* $N\alpha \equiv 0 \pmod{2\pi}$ *and* $|\alpha| < \pi/2$*,*
- *The 1-saddles are the points* $\mathbf{t}_N^{(k)}(\alpha)$ *with* $(N-2)\alpha = \pi \pmod{2\pi}$*,* $|\alpha| < \pi/2$*, and* $k = 1, \ldots, N-1$*.*

Finally, for $N = 2, 3$*, the only sink in* D_N *is the trivial one at* $\boldsymbol{\theta} = \mathbf{0}$*. For* $N = 2$*, the only saddle in* D_N *is* $(0, \pi)$ *and for* $N = 3$ *there are three:* $(0, 0, \pi), (0, \pi, 0), (0, \pi, \pi)$*.*

Corollary 3.2. *If* $N > 4$*,* $N \neq 0 \pmod 4$ *and* $\boldsymbol{\omega} = \mathbf{0}$*, then there are* $1 + 2\lfloor N/4 \rfloor$ *sinks and* $N\lfloor N/4 \rfloor$ *saddles in the fundamental domain* D_N*. In particular, for* $N > 4$*, the system has multiple sinks in* D_N*.*

Proof. First consider the sinks, and assume that $0 < \alpha < \pi/2$. We have

$$N\alpha = 2\pi\ell, \quad 0 < \alpha < \pi/2, \quad \ell \in \mathbb{Z}, \tag{21}$$

or $\ell < \frac{N}{4}$. Since we always choose $N \neq 0 \pmod 4$, we have $\ell = 1, \ldots, \lfloor N/4 \rfloor$, giving $\lfloor N/4 \rfloor$ fixed points. The symmetry $\alpha \to -\alpha$ gives twice as many points, and we single-count the $\alpha = 0$ fixed point.

For the 1-saddles, we similarly want to solve the equation $N\alpha = \pi \pmod 2\pi$ with $0 < \alpha < \pi/2$, so we need to find $\ell \in \mathbb{Z}$ with

$$\frac{(2\ell+1)\pi}{N-2} < \frac{\pi}{2}.$$

Algebraic manipulations give us that $\ell < N/4 - 1$, but note that we can choose $\ell = 0$, so we have $\lfloor N/4 \rfloor$ choices of α. Note also that once we have chosen α, we have N choices for the location of the gap, meaning that we obtain a total of $N\lfloor N/4 \rfloor$ points. We do not double-count the $\alpha \to -\alpha$ symmetry, since $\mathbf{t}_N^{(N-k)}(-a) = \mathbf{t}_N^{(k)}(\alpha)$.

□

Remark 3.3. *Defining* V *as in* (19)*, if* $N\alpha \equiv 0 \pmod{2\pi}$*, then*

$$V(\mathbf{s}_N(\alpha)) = K\left[N - \sum_{k=1}^{N}\cos(\alpha)\right] = KN(1 - \cos(\alpha)). \tag{22}$$

Thus the origin has the lowest energy of any sink and for ϵ small, (5) will spend most of its time in a neighborhood of $[\mathbf{0}]$. The question which remains is to determine how long we expect transitions between elements of $[\mathbf{0}]$.

From the theorem above, the situation is quite simple for $N < 4$: there is one sink in the fundamental torus, and there is either a unique saddle or multiple saddles with the same energy. For $N > 4$, there are multiple sinks, so the pathways can be complicated. In fact, we show that all transitions are basically governed as follows:

Theorem 3.4. *Consider* $N > 4$*,* $N \neq 0 \pmod 4$*, and* $\boldsymbol{\omega} = \mathbf{0}$*. The most likely path from the origin to any translate is a concatenation of paths of the form*

$$\mathbf{0} \to \mathbf{t}_N^{(k_1)}\left(\frac{\pi}{N-2}\right) \to \mathbf{s}_N\left(\frac{2\pi}{N}\right) \to \mathbf{t}_N^{(k_2)}\left(\frac{\pi}{N-2}\right) \to \mathbf{0}', \text{ or}$$
$$\mathbf{0} \to \mathbf{t}_N^{(k_1)}\left(-\frac{\pi}{N-2}\right) \to \mathbf{s}_N\left(-\frac{2\pi}{N}\right) \to \mathbf{t}_N^{(k_2)}\left(-\frac{\pi}{N-2}\right) \to \mathbf{0}',$$

where $\mathbf{0}'$ *is some element of* $[\mathbf{0}]$ *and* k_1, k_2 *are integers. In particular, this means that the timescale of transition is governed by the action*

$$I_N := K\left[N - (N-1)\cos\left(\frac{\pi}{N-2}\right) + \cos\left(\frac{N-3}{N-2}\pi\right)\right], \tag{10}$$

i.e. if τ is the first-passage time from the origin to one of its translates, then

$$\tau \asymp e^{I_N/\epsilon}.$$

Remark 3.5. *Notice that*

$$\frac{I_N}{K} \to 2 + \frac{\pi^2}{2N} + O(N^{-2}), \tag{23}$$

so that for N sufficiently large, the switching timescale is roughly $e^{2K/\epsilon}$. In particular, note that it does not become more difficult for the system to switch as more oscillators are added. Moreover, when $N \to \infty$, $V(\mathbf{s}_N\,(2k\pi/N)) = K\frac{2k\pi}{N} + O(N^{-3}) \to 0$, so that the depth of the asynchronous solutions gets close to the synchronous solution at zero, even though the action of the saddle is always bounded below by 2. See Figure 3 for a schematic figure of the type of potential landscape a path sees. As N gets large, the middle well becomes about as deep as the two outer wells, so that the system (for large N) will spend about as much time there. However, even as $N \to \infty$, the height of the saddles is bounded below by 2.

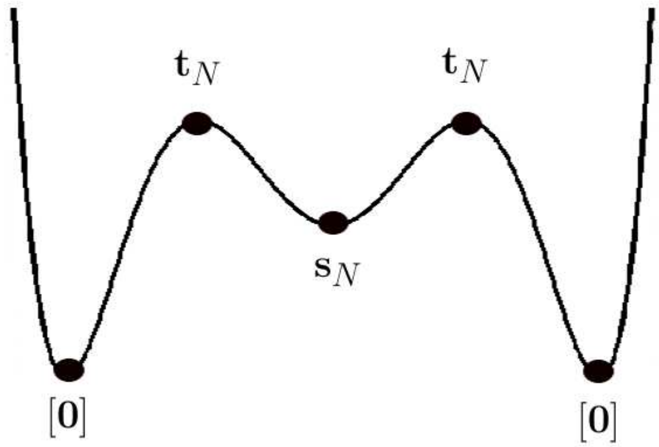

Figure 3: Schematic figure for the minimum energy path

The above statements are specific to $\boldsymbol{\omega} = \mathbf{0}$. What we want to establish here is that for each $N \neq 0 \pmod 4$, there is an open set $\Omega_N \ni \mathbf{0}$ such that Theorems 3.1 and 3.4 still hold, with minor modifications in the statements. The statements of these theorems will be complicated by the fact that while we can be assured that the fixed points and connecting paths exist as they do in those theorems, we will no longer have a formula for these points. We first fix some notation.

Definition 3.3. *Let $\mathbf{x}$ be a fixed point for* (5) *with $\boldsymbol{\omega} = \mathbf{0}$. If $\mathbf{x}$ is hyperbolic, then for an open set of $\boldsymbol{\omega}$ containing $\mathbf{0}$, there is a fixed point of* (6) *with the same index as $\mathbf{x}$ which moves continuously to $\mathbf{x}$ as $\boldsymbol{\omega} \to \mathbf{0}$. We define $\mathbf{x}(\boldsymbol{\omega})$ to be this point for all $\boldsymbol{\omega}$ in this open set, and undefined otherwise; we will also say that $\mathbf{x}(\boldsymbol{\omega})$* **is the point corresponding to** $\mathbf{x}$.

We can now state the theorem which we prove below in Section 4.

Theorem 3.6. *For each $N \neq 0 \pmod 4$, there is an open set Ω_N such that for any fixed point $\mathbf{x}$ described in Theorem 3.1, and for all $\boldsymbol{\omega} \in \Omega_N$, $\mathbf{x}(\boldsymbol{\omega})$ is defined and $\mathbf{0}(\boldsymbol{\omega})$ remains the lowest energy sink. Moreover, all most-likely pathways from $\mathbf{0}$ to $\mathbf{0}'$ are of the form analogous to those in Theorem 3.4, namely*

$$\mathbf{0} \to \mathbf{t}_1 \to \mathbf{s} \to \mathbf{t}_2 \to \mathbf{0}',$$

where $\mathbf{t}_i$ are points corresponding to $\mathbf{t}_N^{(k_i)}\,(\pm\pi/(N-2))$ for some k_i and $\mathbf{s}$ is the point corresponding to $\mathbf{s}_N\,(\pm 2\pi/N)$ (choosing the same sign throughout).

It looks as if little changes when $\boldsymbol{\omega}$ is pushed off of $\mathbf{0}$, and this is more or less true, but some caveats exist. First note that in the case of Theorem 3.4, all of the pathways exhibited have the same total action; more specifically, the energy of the points $\mathbf{t}_N^{(k_i)}\,(\pm\pi/(N-2))$ are independent of choice of k_i, and the system is symmetric. In contrast, a choice of $\boldsymbol{\omega}$ can bias certain pathways due to asymmetry due to lowering the height of particular saddles with respect to others. Moreover, notice that when $\boldsymbol{\omega} \neq \mathbf{0}$, while the differential equations (6) are invariant under a $2\pi\mathbb{Z}^N$ action, the potential (18) is not. The effect of this is to lower the energy of certain members of $[\mathbf{0}]$ with respect to others, which will lead to a long-term "diffusive drift" in the system. These two effects are related but distinct, as we now discuss.

For example, if $\boldsymbol{\omega} = \mathbf{0}$, and we start the system at $\boldsymbol{\theta} = 0$, then it is just as likely to hit any of the saddles $\mathbf{t}_N^{(k)}(\pi/(N-2))$ for $k = 0, \dots, N$ as the other. However, once $\boldsymbol{\omega} \neq \mathbf{0}$, the perturbed saddles inside the fundamental domain can all have different energy and this can bias the system in a certain direction. To see the effect of this tilting, choose $\boldsymbol{\omega}(s)$ some curve in the parameter space. Define $\boldsymbol{\theta}^*(\boldsymbol{\omega}(s))$ as a continuous curve of fixed points as $\boldsymbol{\omega}$ varies as a 1-parameter family. Notice that, by definition,

$$\nabla_{\boldsymbol{\theta}} V(\boldsymbol{\theta}^*(\boldsymbol{\omega}(s)), \boldsymbol{\omega}(s)) = 0 \text{ for all } s \tag{24}$$

so then we have

$$\frac{d}{ds} V(\boldsymbol{\theta}^*(\boldsymbol{\omega}(s)), \boldsymbol{\omega}(s)) = \nabla_{\boldsymbol{\omega}} V(\boldsymbol{\theta}^*(\boldsymbol{\omega}(s)), \boldsymbol{\omega}(s)) \cdot \boldsymbol{\omega}'(s) = -\boldsymbol{\theta}^*(\boldsymbol{\omega}(s)) \cdot \boldsymbol{\omega}'(s).$$

If we consider, for example, a curve $\boldsymbol{\omega}(s)$ with $\boldsymbol{\omega}(s) = \mathbf{0}$, then it is easy to see the effect of a perturbation in $\boldsymbol{\omega}$; we simply take the inner product of the particular fixed point $\boldsymbol{\theta}^*(\mathbf{0})$ we are interested in (and for which we have an explicit representation) with the direction in which we perturb. For example, it might be of interest to compute which $\boldsymbol{\omega}$ give rise to a system which prefers $\mathbf{t}_N^{(k)}(\pi/(N-2))$ for some fixed k, and it is easy to see how to determine these $\boldsymbol{\omega}$ asymptotically. As a specific example, when $\boldsymbol{\omega} = \mathbf{0}$, there are five 1-saddles which limit on $[\mathbf{0}]$, namely

$$\pi/3(0,-4,-3,-2,-1), \quad \pi/3(0,1,-3,-2,-1), \quad \pi/3(0,1,2,-2,-1), \quad \pi/3(0,1,2,3,-1), \quad \pi/3(1,2,3,4).$$

Only one of these is in the fundamental domain D_N. Depending on which entries of $\boldsymbol{\omega}'(\mathbf{0})$ are largest, this will increase or decrease the relative heights of these saddles, biasing the direction in which $\mathbf{0}$ will first jump.

In a related but different issue, the potential is in general no longer invariant under the action of the group $2\pi\mathbb{Z}^N$; in short, the system will now have a preferred direction. For example, consider $\boldsymbol{\omega}$ with $\omega_k > 0$; we then have $V_{\boldsymbol{\omega}}(\boldsymbol{\theta} + 2\pi\mathbf{e}_k) < V_{\boldsymbol{\omega}}(\boldsymbol{\theta})$, meaning that the system is biased to move in the positive θ_k direction. Here the pathway from one element of $[\mathbf{0}]$ to another becomes asymmetric, and we would be more prone to move in one direction than another.

Of course, this argument gives no estimate on the set Ω_N, even about its size. These questions can be approached by other techniques beyond the scope of this paper, and will be considered in detail by this author and collaborators in future work.

4 Proof of Theorems

Here we state the proofs of Theorems 3.1, 3.4, 3.6.

4.1 Proof of Theorem 3.1.

The approach to prove Theorem 3.1 is relatively straightforward: we need to identify all of the fixed points of the system, check that they are hyperbolic, and check their index.

Lemma 4.1. *Choose N with $N \neq 0 \pmod 4$. Choose $k = 0, \dots, N$, $k \neq N/2$, $S \subseteq \{1, \dots, N\}$ with $|S| = k$, and $\ell \in \mathbb{Z}$. Then define*

$$\alpha = \begin{cases} \frac{2\pi\ell}{N-2k}, & k \text{ even}, \\ \frac{(2\ell+1)\pi}{N-2k}, & k \text{ odd}, \end{cases}$$

and define

$$\theta_{n+1} - \theta_n = \begin{cases} \alpha, & k \notin S, \\ \pi - \alpha, & k \in S. \end{cases}$$

Then $\boldsymbol{\theta}$ is a fixed point of (6). Conversely, every fixed point of (6) for $N \neq 0 \pmod 4$ is in the form above, or is a $2\pi\mathbb{Z}^{N-1}$-translate of one of these.

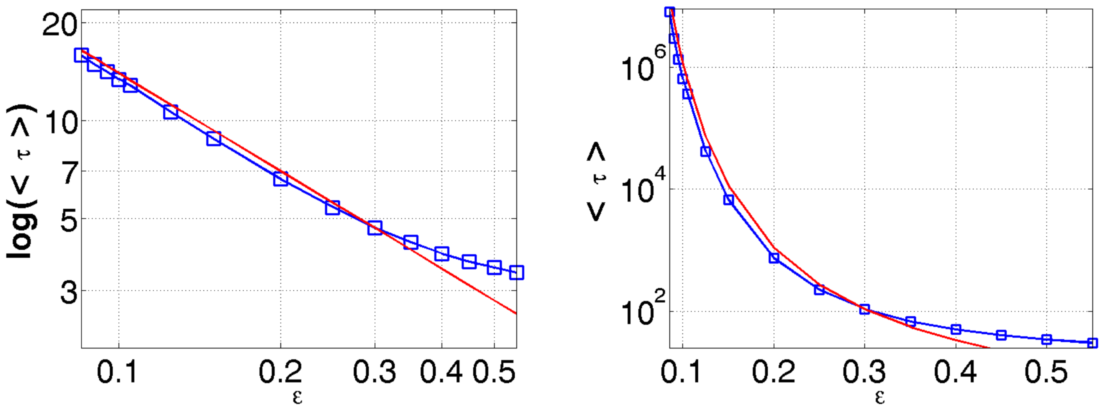

Figure 4: Plot of mean switching times versus ϵ for $N = 5$, $K = 0.2$. We are plotting the same data in both pictures; in frame (a) we plot the logarithm of the mean transition time (blue squares) versus $1.4\epsilon^{-1}$ (rd line) on a log-log plot; in frame (b) we plot the mean transition time versus $e^{1.4/\epsilon}$ on a semilog plot. According to Theorem 3.4, the mean transition time τ satisfies $\tau \asymp e^{1.4/\epsilon}$ as $\epsilon \to 0$; that is to say, the curves should be the same up to a constant factor as $\epsilon \to 0$.

In contrast, if $N = 0 \pmod 4$, then any point in the one-parameter family given by

$$\theta_k = \begin{cases} 0, & k = 0 \pmod 4), \\ \pi, & k = 2 \pmod 4), \\ \alpha, & k = 1 \pmod 2), \end{cases}$$

where $\alpha \in [0, 2\pi]$, is a fixed point for (6), in addition to those described above.

Proof. We write $\eta_n = \theta_{n+1} - \theta_n$. From (6), $\sin(\eta_n) = \sin(\eta_{n-1})$, so that there is an $\beta \in [-1, 1]$ with $\sin(\eta_n) = \beta$ for all n. There is of course the added constraint that

$$\sum_{n=1}^{N} \eta_n = 0 \pmod{2\pi}. \tag{25}$$

Therefore we have the following set of constraints: there exists a number $\alpha \in [-\pi, \pi]$ such that

$$\eta_n = \alpha \wedge \pi - \alpha, \quad \sum_{n=1}^{N} \eta_n = 0 \pmod{2\pi}. \tag{26}$$

The condition we have on α depends on how many of each choice we make. So let us assume that k of the η's are $\pi - \alpha$, and $N - k$ are α. Then the constraint reads

$$(N - k)\alpha - k(\pi - \alpha) = 0 \pmod{2\pi},$$

or

$$(N - 2k)\alpha = k\pi \pmod{2\pi}. \tag{27}$$

If $N \neq 0 \pmod 4$, then either $N = 2 \pmod 4$ and $k = N/2$, or the coefficient of α in (27) is nonzero. This leads to the definition of α as given above, and notice that the k gaps of size $\pi - \alpha$ can be arranged in any order, and this gives all fixed points described above.

If $N = 2 \pmod 4$ and $k = N/2$, then k is odd, so this equation reads $0 = k\pi \pmod{2\pi}$, which has no solution.

Finally, if $N = 0 \pmod 4$, and we choose $k = N/2$, then (27) is solved by any $\alpha \in \mathbb{R}$. The reason that we obtain a continuum of fixed points is due to the fact that $\sin\alpha = \sin(\pi - \alpha)$ for all α; for example, consider $N = 4$, then the one-parameter family $(0, \alpha, \pi, \pi + \alpha)$ works for any α, since the gaps are then $\boldsymbol{\eta} = (\alpha, \pi - \alpha, \alpha, \pi - \alpha)$, and for every term in this sequence, $\sin(\eta_i)$ are the same. □

Remark 4.2. *We can see from the proof that the case of N where $4|N$ is special due to the fact that the saddles are no longer isolated points, but are now one-dimensional manifolds of saddles with a "soft" direction. The FW theory can deal with scenarios such as this [76, Chapter 6] but this would complicate the current picture considerably so we omit it in this paper. However, note that the generic $\boldsymbol{\omega}$ near $\mathbf{0}$ would break this symmetry, so these problems could be studied by the approach taken in this paper.*

Proof of Theorem 3.1. Recalling the construction described in Lemma 4.1, if we show that the sinks are those points obtained by choosing $k = 0$ and $|\alpha| < \pi/2$, and those points obtained by choosing $k = 1$ and $|\alpha| < \pi/2$ give 1-saddles, then we are done. For $N = 2, 3$ and using Lemma 4.1, we can compute all the fixed points and their index by hand, and the reader can see we obtain the result. So we only need consider $N > 4$.

The coordinates of the vector field are given by

$$f_n = \sin(\theta_{n+1} - \theta_n) + \sin(\theta_{n-1} - \theta_n)$$

and thus if J is the Jacobian matrix evaluated at our fixed point,

$$\begin{aligned} J_{i,i+1} &= \frac{\partial f_i}{\partial \theta_{i+1}} = \cos(\theta_{i+1} - \theta_i) = \cos(\eta_i), \\ J_{i,i} &= \frac{\partial f_i}{\partial \theta_i} = -(\cos(\theta_{i+1} - \theta_i) + \cos(\theta_{i-1} - \theta_i)) = -(\cos(\eta_i) + \cos(\eta_{i-1})), \\ J_{i,i-1} &= \frac{\partial f_i}{\partial \theta_{i-1}} = \cos(\theta_{i-1} - \theta_i) = \cos(\eta_{i-1}). \end{aligned}$$

Notice, of course, that since $\theta_0 = 0$, we have $\eta_0 = \theta_1$ and $\eta_{N-1} = -\theta_{N-1}$. J is symmetric and thus has real eigenvalues. Since $\sin(\eta_i) = \beta$ for all i, we have $\cos(\eta_i) = \pm\sqrt{1-\beta^2}$, and we choose plus iff $\eta_i \in (-\pi/2, \pi/2)$.

First consider the case $k = 0$. It is easy to see that we then have

$$J = \pm\sqrt{1-\beta^2}\Delta_N,$$

where Δ_N is the discrete Laplacian with Dirichlet eigenvalues and we choose the plus sign when $|\alpha| < \pi/2$. It is easy to see (e.g. from Gershgorin's Theorem) that Δ_N has all negative eigenvalues.

Now consider $k = 1$, so that we have $N - 1$ gaps of size α and one of size $\pi - \alpha$. Assume WLOG that $\eta_1 = \pi - \alpha$, so that

$$J = \sqrt{1-\beta^2}(\Delta_N + P),$$

where P is the rank-one matrix xx^t, with $x = \sqrt{2}(1, -1, 0, 0, \dots)$. Using Weyl's Inequality [96, 97], we know that the eigenvalues of Δ_N and $\Delta_N + P$ interlace, i.e. if $0 = \lambda_1 > \lambda_2 > \cdots > \lambda_N$ are the eigenvalues of Δ_N, and $\mu_1 \geq \cdots \geq \mu_N$ are the eigenvalues of $\Delta_N + P$, then $\mu_i \geq \lambda_i \geq \mu_{i+1}$. Thus $\Delta_N + P$ has at most one nonnegative eigenvalue. To see that it must have one positive one, it is easy to compute that $\det(\Delta_N + P) = (-1)^{N-1}(N-1)$ which means that it has an odd number of positive eigenvalues (and no zeros). Thus J has exactly one positive eigenvalue.

□

4.2 Proof of Theorem 3.4.

In Theorem 3.1, we have identified the sinks and 1-saddles. We will first show that the 1-saddles with minimum energy are exactly those which appear in the path in Theorem 3.4, and, second, that these saddles do connect the sinks as stated. Since these are connecting paths, and there is no saddle with lower energy, these must be the minimum energy paths.

Lemma 4.3. *The 1-saddles with minimum energy are the points $\mathbf{t}_N^{(k)}\left(\frac{\pi}{N-2}\right)$ for $k = 1, \dots, N$.*

Proof. From Theorem 3.1, we know all 1-saddles are of the form $\mathbf{t}_N^{(k)}(\alpha)$ where $(N-2)\alpha = \pi \pmod{2\pi}$ and $|\alpha| < \pi/2$. In particular, this means that we choose

$$\alpha = \frac{2\ell+1}{N-2}, \quad |\ell| = 1, \dots, \lfloor N/4 \rfloor - 1. \tag{28}$$

We need consider only $\ell > 0$ since $V(-\boldsymbol{\theta}) = V(\boldsymbol{\theta})$. We compute:

$$V(\mathbf{t}_N^{(k)}(\alpha)) = N - (N-1)\cos(\alpha) - \cos(\pi - \alpha), \tag{29}$$

and

$$\frac{\partial V(\mathbf{t}_N^{(k)}(\alpha))}{\partial \alpha} = (N-2)\sin(\alpha) \tag{30}$$

and thus this is an increasing function for $\alpha \in (0, \pi)$. Therefore if we choose $\alpha = (2\ell+1)/(N-2)$ for ℓ a positive integer, then this is an increasing function in ℓ as long as $2\ell + 1 < N - 2$, i.e. $\ell < N/2 - 3/2$, but we only need to consider those points with $\ell < N/4 - 1$, and $N/4 - 1 < N/2 - 3/2$ if $N > 2$.

□

Lemma 4.4. *The unstable manifold of* $\mathbf{t}_N^{(k)}\left(\frac{\pi}{N-2}\right)$ *limits on* $\mathbf{s}_N\left(\frac{2\pi}{N}\right)$ *in one direction and the point* $2\pi f_k$ *in the other.*

Proof. Since $\mathbf{t}_N^{(k)}\left(\frac{\pi}{N-2}\right)$ is a 1-saddle, to prove the lemma we just need to show that there exist two different perturbations of this point which lead to $\mathbf{s}_N\left(\frac{2\pi}{N}\right)$ and $2\pi f_k$ respectively. It is clear by symmetry that if we show the statement of the theorem for $k = 1$, then it holds for all k. Recall that $\mathbf{t}_N^{(1)}\left(\frac{\pi}{N-2}\right)$ has coordinates

$$\theta_0 = 0, \quad \theta_1 = \frac{N-3}{N-2}\pi, \quad \theta_2 = \pi, \quad \theta_k = \pi + \frac{k-2}{N-2}\pi, \quad k > 2.$$

Our two perturbations will be to "kick" θ_1, i.e. we take this point, replace θ_1 with $\theta_1 \pm \epsilon$, and then consider the long-time behavior of that initial condition. We claim that if we kick θ_1 in a positive direction, then it will limit on $2\pi f_k$, and if we kick it in a negative direction, it limits on $\mathbf{s}_N\left(\frac{2\pi}{N}\right)$.

To understand these dynamics, first note the following: Fix θ_{i-1} and θ_{i+1} and do not allow them to move. If $|\theta_{i+1} - \theta_{i-1}| \neq \pi$, then there is a unique (up to 2π-periodicity) fixed point for θ_i, namely the arithmetic mean of its neighbors. If $\theta_{i+1} - \theta_{i-1} < \pi$, this fixed point is attracting, and if $\theta_{i+1} - \theta_{i-1} > \pi$, then this fixed point is repelling. If $\theta_{i+1} - \theta_{i-1} = \pm\pi$, then every point is fixed for θ_i. To see this, notice that

$$\theta_i' = \sin(\theta_{i+1} - \theta_i) + \sin(\theta_{i-1} - \theta_i).$$

Choosing $\theta_i = 1/2(\theta_{i+1} + \theta_{i-1})$ will clearly fix θ_i. Writing $\theta_{i+1} - \theta_{i-1} = q$ with $q \in [0, 2\pi)$, we see that the derivative of the right-hand side is $-2\cos(q/2)$ which is negative iff $q/2 \in (0, \pi/2)$. Finally, since $\sin(\theta) = \sin(\pm\pi - \theta)$, if $\theta_{i+1} - \theta_{i-1} = \pm\pi$ then all θ_i are fixed.

If $\theta_{i+1} - \theta_{i-1} < \pi$, then θ_i is pulled toward the midpoint; if $\theta_{i+1} - \theta_{i-1} < \pi$, then θ_i is repelled from the midpoint and will approach the closer neighbor, and if $\theta_{i+1} - \theta_{i-1} = \pm\pi$, then θ_i can be at rest anywhere. It is also easy to see that if points are lexicographically ordered on the circle, they cannot switch this order, i.e. if $\theta_{i-1}(0) < \theta_i(0) < \theta_{i+1}(0)$ and $\theta_{i+1}(t) - \theta_{i-1}(t) < \pi$, then $\theta_i(t) \in (\theta_{i-1}(t), \theta_{i+1}(t))$. The reason is because if it is attracted to the midpoint it can never match with either neighbor with a larger derivative.

We can now understand the dynamics of perturbations of these fixed points. Consider $\mathbf{t}_N^{(1)}\left(\frac{\pi}{N-2}\right)$ but we now move θ_1 to $\theta_1 + \epsilon$. Since $\theta_2 - \theta_0 = \pi$, θ_1 is happy to stay where it is. However, since θ_1 is now closer to θ_2 than θ_3 is, θ_2 will increase. Once θ_2 has increased, we now have $\theta_2 - \theta_0 > \pi$, and $\theta_1 > \theta_2/2$, so θ_1 will be attracted to θ_2. Moreover, it is easy to see that $\theta_1(t)$ will always be less than $\theta_2(t)$: Since we have $\theta_3(t) \in (\pi, 2\pi)$ for all t, then $\theta_2(t)$ is attracted to the midpoint of $\theta_1(t)$ and $\theta_3(t)$, i.e.

$$\frac{\theta_1(t) + \theta_3(t)}{2} < \frac{\theta_1(t)}{2} + \pi, \tag{31}$$

but as long as $\theta_1(t) > 2\pi/3$, this means $\theta_1(t) > \theta_2(t)$.

On the other hand, let us now move θ_1 to $\theta_1 - \epsilon$. Again, θ_1 is happy to sit anywhere in $(0, \pi)$, since $\theta_2 - \theta_0 = \pi$, but now θ_2 is closer to θ_3 than θ_1, so it will decrease. Once it has decreased $\theta_2 - \theta_0 < \pi$ and thus θ_1 is attracted to $\theta_2/2$. By the lexicographic ordering above, and noting that the gap between θ_1 and θ_0 must always be the largest, the only possible long-term behavior of this solution is $\mathbf{s}_N\left(\frac{2\pi}{N}\right)$.

□

Proof of Theorem 3.4. This follows directly from the two lemmas. Lemma 4.4 shows that the connections as described in Theorem 3.4 exist in Γ_1. Lemma 4.3 shows that $\mathbf{t}_N^{(k)}(\pi/(N-2))$ and their translates are are the lowest energy saddles, and thus these must be the lowest energy pathways. □

Remark 4.5. *We can think of these transition paths as the formation of "communities" inside the entire collection of oscillators. For example, when we start all the oscillators at* $\mathbf{0}$*, they are in one synchronous community. The pathway described in the theorem basically says that some sub-collection of these oscillators splits off from the main mass, diffuses around the circle, and rejoins the rest of the mass at the corresponding translated solution in* $[\mathbf{0}]$.

4.3 Proof of Theorem 3.6

Proof. The proof is relatively straightforward using transversality arguments. More specifically, we proceed as follows.

Consider all of the sinks in the fundamental domain, computed in Theorem 3.1 above. If these points are nondegenerate, then the Implicit Function Theorem tells us that there is some open set of $\boldsymbol{\omega}$ such that (6) has the same set of fixed points with the same indices (of course these points will have moved). Consider $\mathbf{s}_N(\alpha) \in D_N$, which is a sink for $\boldsymbol{\omega} = \mathbf{0}$. From the Implicit Function Theorem, there is an open neighborhood $\Omega \ni \mathbf{0}$ such that for every $\boldsymbol{\omega} \in \Omega$, there is a point $(\mathbf{s}_N(\alpha))(\boldsymbol{\omega})$ corresponding to this sink which is also a sink. An analogous statement exists for all of the saddles. In short, unless and until (6) undergoes a bifurcation, all of the points identified in Theorem 3.1 remain. Finally, note that all of these points are nondegenerate as a consequence of the fact that Δ_N and $\Delta_N + P$ are nonsingular in the proof of Theorem 3.1.

Now consider any pathway as stated in Theorem 3.4. To establish such a pathway, we need to show that the sinks are connected, i.e. that the unstable manifold of the saddles in that path do in fact limit on the sinks. However, note that the basin of attraction of any sink is open by definition, and thus has full dimension. From this it follows that any intersection of the unstable manifold of a saddle with this set is transversal, and it must also persist under perturbation.

Finally, the energy of the saddle points change continuously with respect to $\boldsymbol{\omega}$ and therefore the minimum energy 1-saddle in the fundamental domain must be a point corresponding to $\mathbf{t}_N^{(k_i)}(\pm\pi/(N-2))$. Incidentally, it follows from this that the transition times are continuous functions of $\boldsymbol{\omega}$ as well.

□

5 Conclusions

We considered one special case of a Kuramoto oscillator subject to small noise, and determined the transition times and transition pathways of the system using the FW theory. We made several choices above which we now discuss, and also discuss various generalizations of the results here. The two main choices made above were that we chose a nearest-neighbor interaction graph and that we pinned one of the oscillators to remove the continuous symmetry.

The approach above does not fundamentally require that the interaction graph Γ is nearest-neighbor; if we chose any other symmetric graph Γ, the fundamental calculations would be of the same type as those performed above. If we choose a potential function of the form

$$V(\boldsymbol{\theta}) = \sum_{i,j} \beta_{ij} \cos(\theta_i - \theta_j) - \sum_i \omega_i \theta_i,$$

then

$$-\frac{\partial V}{\partial \theta_k} = \omega_k + \sum_{i,j} (\beta_{ij} + \beta_{ji}) \sin(\theta_i - \theta_j).$$

As stated above, we considered the nearest-neighbor case here mostly because it would lead to the richest structures. Considering the other extreme—namely, all-to-all coupling where $\gamma_{ij} = 1$— then we can only have one fixed point in D_N, so that this system has only the one deep well and the transitions are much simpler. (In fact, one can compute explicitly for $\boldsymbol{\omega} = \mathbf{0}$ that the fixed points for the all-to-all case are exactly those points with $\theta_n = 2\pi kn/N$ for some $k \in \mathbb{Z}$ and that every one except $\boldsymbol{\theta} = \mathbf{0}$ is unstable.) Graphs with more edges will tend to have fewer fixed points, since there are more constraints. The nearest-neighbor case we consider here is, with one exception, the sparsest possible connected symmetric graph we can consider, with that exception being an undirected tree. We plan to consider more general interaction graphs in future work. We also point out that we could consider more general coupling between oscillators using the same framework (e.g. replace $\sin(\cdot)$ with an odd function) and this fundamental approach would work as well (although, again, one would have to do different computations).

Any Kuramoto problem in the form (1) has a continuous group symmetry $\boldsymbol{\theta} \mapsto \boldsymbol{\theta} + \alpha\mathbf{1}$, and this is dealt with in a variety of ways in the deterministic setting. We pinned one of the oscillators above, but there are other possibilities: We could consider the diffusion restricted to a given submanifold in $\mathbb{R}^N$, we could consider the flow on the quotient space $\mathbb{R}^N/\{\mathbf{1}\}$, or we could even consider a new coordinate system for $\mathbb{R}^N$ which simplifies the process. As for the first possibility, notice that the deterministic system (6) has the property that the sum $\sum \theta_n$ is always conserved, so that the flow is naturally restricted to a submanifold (in fact, one element of $\mathbb{R}^N/\{\mathbf{1}\}$). The restriction of a diffusion to a submanifold is a well-studied problem [98–100] and in this case we can explicitly compute the effective system. To proceed, we subtract off the mean position of the oscillators during the evolution, namely choose $s = \sum_{n=0}^{N-1} \theta_n$, and define $\zeta_n = \theta_n - s$. We then have

$$\begin{aligned} ds &= \sqrt{2\epsilon} \sum_{n=0}^{N-1} dW_t^{(n)}, \\ d\zeta_n &= \{\omega_n + K\left[\sin(\theta_{n+1} - \theta_n) + \sin(\theta_{n-1} - \theta_n)\right]\}\, dt - \sqrt{2\epsilon} \sum_{k \neq n} dW_t^{(k)}. \end{aligned}$$

If we define $dZ_t^{(k)}$ as this last sum, then $dZ_t^{(k)} \sim^{\mathcal{D}} \sqrt{2\epsilon(N-1)}\, dW_t^{(k)}$ so we can replace $dZ_t^{(k)}$ with a single white-noise process; however, the different noise terms will now be correlated. Of course, there is no problem with applying the FW formalism to the case where we have correlated noises, but as it turns out, the formulas become more complicated. A complimentary idea to the above would be to consider an orthogonal transformation to a coordinate system which respects the foliation of $\mathbb{R}^N$ by elements of $\mathbb{R}^N/\{\mathbf{1}\}$ (there are in fact many choices for this). The advantage in such a case would be that the forcing would still be Brownian motion in $\mathbb{R}^N$ (and thus the components would be independent white noises) but the drift terms would be changed, and in particular would no longer have the nearest-neighbor structure. Another possibility would be to consider the flow on the quotient space $\mathbb{R}^N/\{\mathbf{1}\}$ (see e.g. [101, §36]) but this adds difficulties in notation, at the very least, due to taking two different quotients. Also, the pinning of one oscillator makes the index theory a bit easier since we've removed the soft translation-invariant mode (q.v. the proof of Theorem 3.4).

Finally, we remark that everything done in this paper is in the asymptotic regime where N is fixed (but perhaps large) and $\epsilon \to 0$ for fixed N. As shown above, in this regime the limiting transition is always points of type $\mathbf{t}_N^{(k)}(\pi/(N-2))$ since they have the smallest energy. However, if we consider a case where we fix ϵ small but then take N large, we would expect to see transitions across saddles whenever they got below a certain critical energy, and notice that as $N \to \infty$ the energy of the saddles all converge to 2. Using (29), the barrier as $N \to \infty$ goes like

$$\lim_{N\to\infty} V(\mathbf{t}_N^{(k)}(\alpha)) = N - (N-1)\cos(\alpha) - \cos(\pi - \alpha),$$

and we take $\alpha = \ell\pi/(N-2)$ for some $\ell \in \mathbb{Z}$, we see that we obtain the same asymptotics as in (23). So we would expect, for fixed $\epsilon \ll 1$ and $N \to \infty$, the system can find more complicated transitions. Of course, it is very difficult to make rigorous statements about transitions when one does not take the $\epsilon \to 0$ limit and we do not do so here.

6 Acknowledgments

The author would like to thank Jared Bronski, Eugene Lerman, and Susan Tolman for discussions which improved this article.

References

[1] C. S. Peskin. *Mathematical aspects of heart physiology*. Courant Institute of Mathematical Sciences New York University, New York, 1975. Notes based on a course given at New York University during the year 1973/74, see `http://math.nyu.edu/faculty/peskin/heartnotes/index.html`.

[2] Michael R. Guevara and Leon Glass. Phase locking, period doubling bifurcations and chaos in a mathematical model of a periodically driven oscillator: A theory for the entrainment of biological oscillators and the generation of cardiac dysrhythmias. *Journal of Mathematical Biology*, 1982.

[3] L. Glass, A. L. Goldberger, M. Courtemanche, and A. Shrier. Nonlinear dynamics, chaos and complex cardiac arrhythmias. *Proc. Roy. Soc. London Ser. A*, 413(1844):9–26, 1987.

[4] C. A. Czeisler, E. Weitzman, M. C. Moore-Ede, J. C. Zimmerman, and R. S. Knauer. Human sleep: its duration and organization depend on its circadian phase. *Science*, 210(4475):1264–1267, 1980.

[5] John J. Tyson, Christian I. Hong, C. Dennis Thron, and Bela Novak. A Simple Model of Circadian Rhythms Based on Dimerization and Proteolysis of PER and TIM. *Biophys. J.*, 77(5):2411–2417, 1999.

[6] G. Bard Ermentrout and John Rinzel. Reflected waves in an inhomogeneous excitable medium. *SIAM Journal on Applied Mathematics*, 1996.

[7] Raymond Kapral and Kenneth Showalter, editors. *Chemical Waves and Patterns*. Springer, 1994.

[8] J.P. Keener. Propagation and its failure in coupled systems of discrete excitable cells. *SIAM Journal on Applied Mathematics*, 47(3):556–572, 1987.

[9] John J. Tyson and James P. Keener. Singular perturbation theory of traveling waves in excitable media (a review). *Phys. D*, 32(3):327–361, 1988.

[10] Julyan H. E. Cartwright, Victor M. Eguluz, Emilio Hernndez-Garca, and Oreste Piro. Dynamics of elastic excitable media. *Int. J. of Bifurcation and Chaos*, 9(11):2197–2202, 1999.

[11] Y. Kuramoto. *Chemical oscillations, waves, and turbulence*, volume 19 of *Springer Series in Synergetics*. Springer-Verlag, Berlin, 1984.

[12] J.P. Sethna, K. Dahmen, S. Kartha, J.A. Krumhansl, B.W. Roberts, and J.D. Shore. Hysteresis and hierarchies: Dynamics of disorder-driven first-order phase transformations. *Physical Review Letters*, 70(21):3347–3350, 1993.

[13] Zeev Olami, Hans Jacob S. Feder, and Kim Christensen. Self-organized criticality in a continuous, nonconservative cellular automaton modeling earthquakes. *Phys. Rev. Lett.*, 68(8):1244–1247, Feb 1992.

[14] Maria de Sousa Vieira. Chaos and synchronized chaos in an earthquake model. *Phys. Rev. Lett.*, 82(1):201–204, Jan 1999.

[15] Y. Kuramoto. Collective synchronization of pulse-coupled oscillators and excitable units. *Physica D*, 50(1):15–30, May 1991.

[16] L. F. Abbott and C. van Vreeswijk. Asynchronous states in networks of pulse-coupled oscillators. *Physical Review E*, 48(2):1483–1490, August 1993.

[17] W. Gerstner and J. L. van Hemmen. Coherence and incoherence in a globally-coupled ensemble of pulse-emitting units. *Physical Review Letters*, 71(3):312–315, July 1993.

[18] M. Tsodyks, I. Mitkov, and H. Sompolinsky. Pattern of synchrony in inhomogeneous networks of oscillators with pulse interactions. *Physical Review Letters*, 71(8):1280–1283, August 1993.

[19] C. van Vreeswijk, L. Abbott, and G. Ermentrout. When inhibition not excitation synchronizes neural firing. *J. Comp. Neurosci.*, pages 313–322, 1994.

[20] P. C. Bressloff and S. Coombes. Desynchronization, mode locking, and bursting in strongly coupled integrate-and-fire oscillators. *Physical Review Letters*, 81(10):2168–2171, September 1998.

[21] D. Terman, N. Kopell, and A. Bose. Dynamics of two mutually coupled slow inhibitory neurons. *Phys. D*, 117(1-4):241–275, 1998.

[22] C. van Vreeswijk and H. Sompolinsky. Chaotic balance state in a model of cortical circuits. *Neural Computation*, 10(6):1321–1372, August 15 1998.

[23] S. R. Campbell, D. L. L. Wang, and C. Jayaprakash. Synchrony and desynchrony in integrate-and-fire oscillators. *Neural Computation*, 11(7):1595–1619, October 1999.

[24] D. Hansel and H. Sompolinsky. Synchronization and computation in a chaotic neural network. *Phys. Rev. Lett.*, 68(5):718–721, Feb 1992.

[25] Khashayar Pakdaman and Denis Mestivier. Noise induced synchronization in a neuronal oscillator. *Phys. D*, 192(1-2):123–137, 2004.

[26] John Buck and Elisabeth Buck. Mechanism of rhythmic synchronous flashing of fireflies. *Science*, 1968.

[27] R. E. Mirollo and S. H. Strogatz. Synchronization of pulse-coupled biological oscillators. *SIAM J. Appl. Math.*, 50(6):1645–1662, 1990.

[28] Z.-H. Liu and P.M. Hui. Collective signaling behavior in a networked-oscillator model. *Physica A: Statistical Mechanics and its Applications*, 383(2):714 – 724, 2007.

[29] S. Strogatz. *Sync: The Emerging Science of Spontaneous Order*. Hyperion, 2003.

[30] A. Pikovsky, M. Rosenblum, and J. Kurths. *Synchronization: A Universal Concept in Nonlinear Sciences*. Cambridge University Press, 2003.

[31] Arthur T. Winfree. *The geometry of biological time*, volume 12 of *Interdisciplinary Applied Mathematics*. Springer-Verlag, New York, second edition, 2001.

[32] Y. Kuramoto. Chaos and statistical methods. *Chaos and Statistical Methods*, 1, 1984.

[33] S.H. Strogatz. From Kuramoto to Crawford: exploring the onset of synchronization in populations of coupled oscillators. *Physica D: Nonlinear Phenomena*, 143(1-4):1–20, 2000.

[34] J.A. Acebrón, L.L. Bonilla, C.J.P. Vicente, F. Ritort, and R. Spigler. The Kuramoto model: A simple paradigm for synchronization phenomena. *Reviews of modern physics*, 77(1):137, 2005.

[35] K. Wiesenfeld, P. Colet, and S.H. Strogatz. Synchronization transitions in a disordered josephson series array. *Physical review letters*, 76(3):404–407, 1996.

[36] D. Hansel, G. Mato, and C. Meunier. Clustering and slow switching in globally coupled phase oscillators. *Phys. Rev. E*, 48(5):3470–3477, Nov 1993.

[37] LF Abbott and C. van Vreeswijk. Asynchronous states in networks of pulse-coupled oscillators. *Physical Review E*, 48(2):1483, 1993.

[38] S.M. Crook, G.B. Ermentrout, and J.M. Bower. Spike frequency adaptation affects the synchronization properties of networks of cortical oscillators. *Neural Computation*, 10(4):837–854, 1998.

[39] Pranay Goel and Bard Ermentrout. Synchrony, stability, and firing patterns in pulse–coupled oscillators. *Physica D: Nonlinear Phenomena*, 163(3–4):191–216, 2002.

[40] R. Mirollo and S.H. Strogatz. The spectrum of the partially locked state for the kuramoto model. *Journal of Nonlinear Science*, 17:309–347, 2007. 10.1007/s00332-006-0806-x.

[41] G.B. Ermentrout. Synchronization in a pool of mutually coupled oscillators with random frequencies. *Journal of Mathematical Biology*, 22(1):1–9, 1985.

[42] S.H. Strogatz, R.E. Mirollo, and P.C. Matthews. Coupled nonlinear oscillators below the synchronization threshold: relaxation by generalized Landau damping. *Physical review letters*, 68(18):2730–2733, 1992.

[43] Renato E. Mirollo and Steven H. Strogatz. The spectrum of the locked state for the kuramoto model of coupled oscillators. *Physica D: Nonlinear Phenomena*, 205(1-4):249 – 266, 2005. Synchronization and Pattern Formation in Nonlinear Systems: New Developments and Future Perspectives.

[44] E. A. Martens, E. Barreto, S. H. Strogatz, E. Ott, P. So, and T. M. Antonsen. Exact results for the Kuramoto model with a bimodal frequency distribution. *Phys. Rev. E*, 79(2):026204, Feb 2009.

[45] R. E. Mirollo and S. H. Strogatz. Synchronization of pulse-coupled biological oscillators. *SIAM J. Appl. Math.*, 50(6):1645–1662, 1990.

[46] Y. Maistrenko, O. Popovych, O. Burylko, and PA Tass. Mechanism of desynchronization in the finite-dimensional Kuramoto model. *Physical review letters*, 93(8):84102, 2004.

[47] F. De Smet and D. Aeyels. Partial entrainment in the finite kuramoto-sakaguchi model. *Physica D: Nonlinear Phenomena*, 234(2):81–89, 2007.

[48] O. DHuys, R. Vicente, T. Erneux, J. Danckaert, and I. Fischer. Synchronization properties of network motifs: Influence of coupling delay and symmetry. *Chaos: An Interdisciplinary Journal of Nonlinear Science*, 18:037116, 2008.

[49] E. Canale, P. Monzón, and F. Robledo. Global synchronization properties for different classes of underlying interconnection graphs for Kuramoto coupled oscillators. *Future Generation Information Technology*, pages 104–111, 2009.

[50] F. Dorfler and F. Bullo. On the critical coupling for Kuramoto oscillators. *Arxiv preprint arXiv:1011.3878*, 2010.

[51] D.A. Wiley, S.H. Strogatz, and M. Girvan. The size of the sync basin. *Chaos: An Interdisciplinary Journal of Nonlinear Science*, 16:015103, 2006.

[52] J. Teramae and Y. Kuramoto. Strong desynchronizing effects of weak noise in globally coupled systems. *Physical Review E*, 63(3):036210, 2001.

[53] J. Teramae and D. Tanaka. Robustness of the noise-induced phase synchronization in a general class of limit cycle oscillators. *Physical review letters*, 93(20):204103, 2004.

[54] B.C. Bag, KG Petrosyan, and C.K. Hu. Influence of noise on the synchronization of the stochastic Kuramoto model. *Physical Review E*, 76(5):056210, 2007.

[55] M.G. Rosenblum, A.S. Pikovsky, and J. Kurths. Phase synchronization of chaotic oscillators. *Physical Review Letters*, 76(11):1804–1807, 1996.

[56] C. Zhou, J. Kurths, I.Z. Kiss, and J.L. Hudson. Noise-enhanced phase synchronization of chaotic oscillators. *Physical review letters*, 89(1):14101, 2002.

[57] E. Fermi, J. Pasta, and S. Ulam. Studies of nonlinear problems. *Los Alamos document LA 1940*, 1955.

[58] R. Livi, M. Pettini, S. Ruffo, M. Sparpaglione, and A. Vulpiani. Equipartition threshold in nonlinear large hamiltonian systems: The Fermi-Pasta-Ulam model. *Physical Review A*, 31(2):1039, 1985.

[59] J. Ford. The Fermi-Pasta-Ulam problem: Paradox turns discovery. *Physics Reports*, 213(5):271–310, 1992.

[60] P. Ashwin and JW Swift. The dynamics of N weakly coupled identical oscillators. *Journal of Nonlinear Science*, 2(1):69–108, 1992.

[61] B. Rink and F. Verhulst. Near-integrability of periodic FPU-chains. *Physica A: Statistical Mechanics and its Applications*, 285(3-4):467–482, 2000.

[62] B. Rink. Symmetry and resonance in periodic FPU chains. *Communications in Mathematical Physics*, 218(3):665–685, 2001.

[63] K. Parwani and K. Josić. Rotation sets for networks of circle maps. *Chaos: An Interdisciplinary Journal of Nonlinear Science*, 16:015115, 2006.

[64] J.R. Chazottes and B. Fernandez. *Dynamics of coupled map lattices and of related spatially extended systems*, volume 671. Springer-Verlag New York Inc, 2005.

[65] A. Bovier. Statistical mechanics of disordered systems-series: Cambridge series in statistical and probabilistic mathematics (no. 18). *Statistical Mechanics of Disordered Systems-Series: Cambridge Series in Statistical and Probabilistic Mathematics (No. 18), by Anton Bovier, pp. 324. Cambridge University Press, June 2006. ISBN-10: 0521849918. ISBN-13: 9780521849913*, 1, 2006.

[66] GW Ford, M. Kac, and P. Mazur. Statistical mechanics of assemblies of coupled oscillators. *Journal of Mathematical Physics*, 6(4):504–515, 1965.

[67] H. Spohn and J.L. Lebowitz. Stationary non-equilibrium states of infinite harmonic systems. *Communications in Mathematical Physics*, 54(2):97–120, 1977.

[68] H. Spohn. *Large scale dynamics of interacting particles*, volume 174. Springer-Verlag New York:, 1991.

[69] J.P. Eckmann, C.A. Pillet, and L. Rey-Bellet. Non-equilibrium statistical mechanics of anharmonic chains coupled to two heat baths at different temperatures. *Communications in Mathematical Physics*, 201(3):657–697, 1999.

[70] J.P. Eckmann and M. Hairer. Non-equilibrium statistical mechanics of strongly anharmonic chains of oscillators. *Communications in Mathematical Physics*, 212(1):105–164, 2000.

[71] C.B. Muratov and E. Vanden-Eijnden. Breakup of universality in the generalized spinodal nucleation theory. *Journal of Statistical Physics*, 114(3):605–623, 2004.

[72] R.V. Kohn, M.G. Reznikoff, and E. Vanden-Eijnden. Magnetic elements at finite temperature and large deviation theory. *Journal of Nonlinear Science*, 15(4):223–253, 2005.

[73] R.V. Kohn, F. Otto, M.G. Reznikoff, and E. Vanden-Eijnden. Action minimization and sharp-interface limits for the stochastic allen-cahn equation. *Communications on Pure and Applied Mathematics*, 60(3):393–438, 2007.

[74] M. Hairer and J.C. Mattingly. Slow energy dissipation in anharmonic oscillator chains. *Communications on Pure and Applied Mathematics*, 62(8):999–1032, 2009.

[75] K.K. Lin, E. Shea-Brown, and L.S. Young. Reliability of coupled oscillators. *Journal of Nonlinear Science*, 19(5):497–545, 2009.

[76] Mark I. Freidlin and Alexander D. Wentzell. *Random perturbations of dynamical systems*. Springer-Verlag, New York, second edition, 1998.

[77] M.I. Freidlin and A.D. Wentzell. Diffusion processes on graphs and the averaging principle. *The Annals of Probability*, 21(4):2215–2245, 1993.

[78] A. Bovier, M. Eckhoff, V. Gayrard, and M. Klein. Metastability and small eigenvalues in Markov chains. *Journal of Physics A: Mathematical and General*, 33:L447, 2000.

[79] A. Bovier, M. Eckhoff, V. Gayrard, and M. Klein. Metastability in reversible diffusion processes I. sharp estimates for capacities and exit times. *J. Eur. Math. Soc*, 6:399–424, 2004.

[80] A. Bovier, V. Gayrard, and M. Klein. Metastability in reversible diffusion processes. II. precise asymptotics for small eigenvalues. *J. Eur. Math. Soc.(JEMS)*, 7(1):69–99, 2005.

[81] E. Olivieri and M.E. Vares. *Large deviations and metastability*. Cambridge Univ Pr, 2005.

[82] Adam Shwartz and Alan Weiss. *Large deviations for performance analysis*. Chapman & Hall, London, 1995.

[83] Jean-Dominique Deuschel and Daniel W. Stroock. *Large deviations*, volume 137 of *Pure and Applied Mathematics*. Academic Press Inc., Boston, MA, 1989.

[84] S. R. S. Varadhan. *Large deviations and applications*, volume 46 of *CBMS-NSF Regional Conference Series in Applied Mathematics*. Society for Industrial and Applied Mathematics (SIAM), Philadelphia, PA, 1984.

[85] M.D. Donsker and SRS Varadhan. Asymptotic evaluation of certain Markov process expectations for large time, i. *Communications on Pure and Applied Mathematics*, 28(1):1–47, 1975.

[86] Nils Berglund and Barbara Gentz. *Noise-induced phenomena in slow-fast dynamical systems: A sample-paths approach*. Probability and its Applications (New York). Springer-Verlag London Ltd., London, 2006.

[87] R. E. Lee DeVille, Cyrill B. Muratov, and Eric Vanden-Eijnden. Two distinct mechanisms of coherence in randomly perturbed dynamical systems. *Phys. Rev. E (3)*, 72(3):031105, 2005.

[88] N. Berglund, B. Fernandez, and B. Gentz. Metastability in interacting nonlinear stochastic differential equations: I. from weak coupling to synchronization. *Nonlinearity*, 20:2551, 2007.

[89] N. Berglund, B. Fernandez, and B. Gentz. Metastability in interacting nonlinear stochastic differential equations: II. large-N behaviour. *Nonlinearity*, 20:2583, 2007.

[90] N. Berglund and B. Gentz. The Eyring-Kramers law for potentials with nonquadratic saddles. *Arxiv preprint arXiv:0807.1681*, 2008.

[91] R. E. Lee DeVille and Eric Vanden-Eijnden. A nontrivial scaling limit for multiscale Markov chains. *J. Stat. Phys.*, 126(1):75–94, 2007.

[92] R. E. Lee DeVille and Eric Vanden-Eijnden. Regular gaits and optimal velocities for motor proteins. *Biophysical J.*, 95(6):2681–2691, September 15 2008.

[93] G.S. Medvedev and S. Zhuravytska. The geometry of spontaneous spiking in neuronal networks. *Arxiv preprint arXiv:1105.2801*, 2011.

[94] H. Risken. *The Fokker-Planck equation: Methods of solution and applications*, volume 18. Springer Verlag, 1996.

[95] C.W. Gardiner. Handbook of stochastic methods for physics, chemistry and the natural sciences. *Springer series in synergetics*, 13, 2004.

[96] J.N. Franklin. *Matrix theory*. Dover Pubns, 2000.

[97] Wasin So. Rank one perturbation and its application to the Laplacian spectrum of a graph. *Linear & Multilinear Algebra*, 46:193–198, 1999.

[98] JT Lewis. Brownian motion on a submanifold of euclidean space. *Bulletin of the London Mathematical Society*, 18(6):616, 1986.

[99] D.W. Stroock. Brownian motion on a submanifold. *Communications in analysis and geometry*, 12(1/2):165–182, 2004.

[100] Giovanni Ciccotti, Tony Lelievre, and Eric Vanden-Eijnden. Projection of diffusions on submanifolds: application to mean force computation. *Comm. Pure Appl. Math.*, 61(3):371–408, 2008.

[101] L.C.G. Rogers and D. Williams. *Diffusions, Markov processes, and martingales*, volume 2. Cambridge Univ Pr, 2000.